TMEM97 increases in synapses and is a potential synaptic Aβ binding partner in human Alzheimer's disease

Martí Colom-Cadena, PhD[1], Jane Tulloch, BSc[1], Rosemary J Jackson, PhD[1,2], James H Catterson, PhD,[1] Jamie Rose[1], Caitlin Davies, BSc[1], Monique Hooley, Msc[1], Alejandro Anton-Fernandez, PhD[1], Sophie Dunnett, BSc[1], Robert Tempelaar, MSc[1], Makis Tzioras, MSc[1], Nicholas J Izzo, PhD[3], Susan M. Catalano, PhD[3], Colin Smith, MD, RCPath[4], and Tara L. Spires-Jones, DPhil*[1]

[1] The University of Edinburgh Centre for Discovery Brain Sciences and UK Dementia Research Institute, Edinburgh.
[2] Current address: MassGeneral Institute for Neurodegenerative Diseases, Massachusetts General Hospital, Harvard Medical School, USA.
[3] Cognition Therapeutics Inc., Pittsburgh, PA, USA.
[4] Centre for Clinical Brain Sciences and Sudden Death Brain Bank, University of Edinburgh, Edinburgh.

*Correspondence to
Prof Tara Spires-Jones
Tara.spires-jones@ed.ac.uk
Centre for Discovery Brain Sciences
The University of Edinburgh
1 George Square, Edinburgh EH8 9JZ, UK

One Sentence Summary

In Alzheimer's disease, TMEM97 was present in a higher proportion of synapses and close enough to amyloid beta to be a potential synaptic binding partner.

Abstract

Synapse loss correlates with cognitive decline in Alzheimer's disease (AD), and soluble amyloid beta (Aβ) is implicated in synaptic dysfunction and loss. An important knowledge gap is the lack of understanding of how synaptic accumulation of Aβ leads to synapse degeneration. In particular, there has been difficulty in determining whether there is a synaptic receptor that binds Aβ and mediates toxicity. While many candidate synaptic binding partners have been observed in model systems, their relevance to human AD brain remains unknown. This is in part due to methodological limitations preventing visualization of Aβ binding at individual synapses. To overcome this limitation, we combined two high resolution microscopy techniques: array tomography and Förster resonance energy transfer (FRET) to image over 1 million individual synaptic terminals in temporal cortex from AD (n=9) and age matched control cases (n=6). Within postsynaptic densities, Aβ generates a FRET signal with transmembrane protein 97 (TMEM97), recently discovered to be the Sigma-2 receptor, cellular prion protein, and postsynaptic density 95 (PSD95). TMEM97 is also present in a higher proportion of postsynapses in AD brain compared to control. Further, we inhibited Aβ-TMEM97 interaction in the APP/PS1+Tau mouse model of AD by treating with the Sigma-2 receptor complex allosteric antagonist CT1812 (n=20) or vehicle (n=20). CT1812 drug concentration correlated negatively with synaptic FRET signal between TMEM97 and Aβ. These data support a role for TMEM97 in the synaptic binding of Aβ in human Alzheimer's disease brain where it may mediate synaptotoxicity.

Introduction

In Alzheimer's disease (AD), synapse loss is an early event in the aetiology of the disease and is the best pathological correlate of cognitive decline *(1–3)*. The mechanism(s) underlying synapse degeneration, however, are still largely unknown *(4)*. We and others have observed that oligomeric amyloid beta (Aβ) peptide causes synaptic dysfunction, accumulates within in synapses, and is associated with synapse loss around plaques *(5–9)*. While it is clear that toxicity of tau and changes in non-neuronal cells are also important in disease pathogenesis *(10)*, substantial evidence supports an important role for Aβ in synaptotoxicity and early AD pathogenesis *(11)*. As such, it is important to identify synaptic binding partners of Aβ which may mediate synaptotoxicity in human brain. Disrupting binding of Aβ with synaptic receptors is a promising therapeutic avenue as such interactions are "druggable", or able to be interrupted with standard pharmacological approaches *(12)*.

Synaptic Aβ binding partners have been identified in cell culture systems and mouse models, but their human relevance is still debated, reviewed in *(13–16)*. Among the Aβ binding candidates, cellular prion protein (PrP_c) represents the most studied, either alone or through a complex with mGluR5 *(17–20)*. Other suggested Aβ binding partners at synapses include the α7-nicotinic receptor *(21)*, Ephrin A4 (EphA4) *(22)*, PSD95 *(7, 23, 24)* and LilrB2 *(25)*. An important outstanding question in the field is which of these potential partners binds Aβ in human synapses, as most binding partners have not been validated in AD cases nor using human derived Aβ species *(11, 16)*.

TMEM97, transmembrane protein 97, is a promising potential synaptic binding partner of Aβ. TMEM97 was recently identified as the gene that codes for the Sigma-2 receptor *(26)*. Sigma-2 receptors have been known for more than four decades and are drug targets for several

conditions including cancer, pain and diverse CNS disorders *(27, 28)*. In the context of AD, in 2014, Izzo and colleagues found that Sigma-2 antagonists could improve cognitive deficits in a mouse model of AD *(29, 30)* and could displace Aβ synthetic oligomers from their synaptic receptors in cellular models *(31)*. More recently, a Sigma-2 antagonist has entered clinical trials for AD treatment *(32, 33)*. Little is known about the pathophysiological role of Sigma-2, especially due its unknown identity until the identification of TMEM97. TMEM97, initially known as MAC30 *(34)*, is overexpressed in some cancers and it is believed to be a key player of cholesterol homeostasis *(35)* and calcium regulation *(30, 36, 37)*. Linking this function to AD, in cellular models, TMEM97 has recently been shown to form a ternary complex with PGRMC1 and LDLR *(38)* that may control the internalization of monomers and oligomers of Aβ *(39)*. In addition, our group recently found increased levels of TMEM97 in synaptoneurosomes from AD cases in a proteomics study *(40)*, supporting a potential role in synaptotoxicity in humans. However until this study, it was not known whether TMEM97 and Aβ are found within the same synapses in human brain and whether they are in close enough proximity to be binding partners.

The study of synapses in the human brain represents a technical challenge due to their small volumes, which are smaller than the diffraction limit of light microscopy, making colocalization studies difficult. In the present work we applied a new approach for the study of the close proximity of proteins in synapses in human postmortem brain tissue. To visualize the potential interaction between Aβ and potential binding partners at synapses, we combined array tomography *(41)* and Föster resonance energy transfer (FRET) microscopy *(42, 43)*. Array tomography allows us to reach a 70nm axial resolution, which enables the identification of single synaptic terminals in three dimensions *(44)*. The combination of array tomography with FRET enhances the lateral resolution to ~10nm in the selected single synaptic terminals allowing us to determine whether proteins are close enough to be interacting *(7, 45)*.

Our current study demonstrates that TMEM97 is a potential Aβ synaptic binding partner in human brain tissue and confirms that Sigma2 receptor complex allosteric antagonist CT1812 can reduce interactions between TMEM97 and Aβ in vivo. These findings may be of help for AD therapeutic approaches and also contribute to a technical advance in the study of the still elusive synaptic structures involved in neurodegeneration.

Results

Demographic, clinical, neuropathological and genetic characteristics of human cases

We used human post-mortem brain samples from inferior temporal gyrus (BA20/21) to investigate proximity of Aβ and synaptic proteins. Details of human cases included are shown in **Table 1**. Our AD and control cohorts are age and sex matched (p>0.05, Wilcoxon and Fisher-exact test, respectively). *APOE* e4 carriers were more common in AD than in the control group (Fisher-exact test, p=0.028). Post-mortem interval (PMI) was slightly longer in AD group (Welch's t-test, p=0.049). Both sex and PMI were included as a covariates in the statistical analyses of the study.

Case	BBN	Diagnosis (clinical)	*APOE* genotype	Brain weight (g)	Age at death (y)	Sex	PMI (h)	Braak NFT stage	Thal Aβ phase
1	001.28406	control	3/3	1437	79	m	72	II	2
2	001.28794	control	2/3	1289	79	f	72	I	0
3	001.26495	control	3/3	1290	78	m	39	I	1
4	001.28797	control	3/3	1301	79	m	57	0	0
5	001.29086	control	3/3	1468	79	f	68	0	1
6	BBN_19686	control	3/3	1320	77	f	75	I	1
7	001.29695	AD	3/4	1300	86	m	72	VI	5
8	001.28771	AD	3/3	1183	85	m	91	VI	5
9	001.32929	AD	3/3	1354	85	f	80	VI	5
10	BBN_25739	AD	3/4	1375	85	f	45	VI	5
11	001.35096	AD	3/4	1209	72	m	103	VI	5
12	001.30973	AD	3/4	1210	89	f	96	VI	5
13	001.26718	AD	3/4	1367	78	m	74	VI	5
14	BBN_24322	AD	3/4	1410	80	m	101	VI	5
15	BBN_24527	AD	3/3	1160	81	m	74	V	4

Table 1. Demographic, clinical, neuropathological and genetic data of human cases. AD: Alzheimer's disease; NFT: neurofibrillary tangle; PMI: postmortem interval, BBN: Medical Research Council Brain Bank number.

TMEM97 levels are increased in AD

The overall density of TMEM97 positive objects was assessed in the temporal cortex revealing an immunoreactivity pattern of a membrane protein, with widespread presence in grey matter in both AD and control cases (**Fig. 1A**). The density of TMEM97 objects was significantly higher in AD than control cases (fold increase: 1.52; $\beta = 2.04 \times 10^{10}$; p=0.007). This increase was not related to the proximity of an Aβ plaque (**Fig. 1B**). As previously described *(5)*, postsynaptic terminal density was reduced in the vicinity of Aβ plaque cores of AD cases, although no overall loss was observed when compared with control cases (**Fig. 1C**). As expected, Aβ was more common in AD cases and the density of objects was elevated close to the core of Aβ plaques (fold increase: 2.5; β=77.54; p=0.022; **Fig. 1D**).

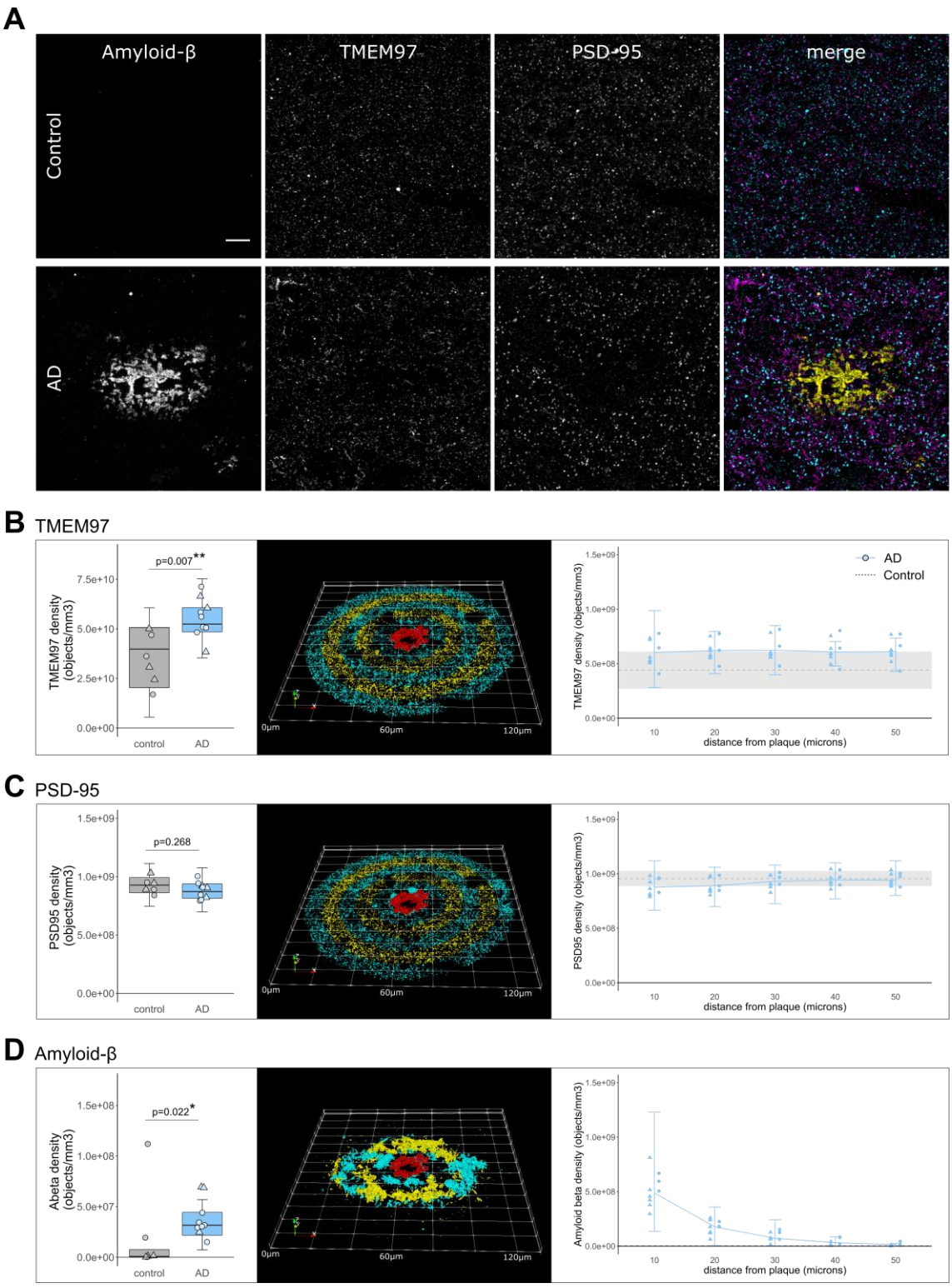

Fig. 1. Immunoreactivity pattern and density of TMEM97, Aβ and PSD95. **A**, representative maximum intensity projection images of 10 consecutive 70nm-thick sections from a control and an AD case. Immunoreactivity against Aβ (yellow), TMEM97 (magenta) and PSD95 (cyan) is shown. Overall density (left) or the density in relation to Aβ plaque cores (right) of TMEM97 (**B**), PSD95 (**C**) and Aβ (**D**) is plotted. The 3D reconstructions were made from 19 consecutive sections of a representative AD case. The Aβ core is shown in red and the objects distributed every 10um bins are coloured. Scale bar represents 10µm. Boxplots show quartiles and medians calculated from all image stacks in the study. Data points show case means (females, triangles; males, circles). Analysis was with linear mixed effects models including diagnostic group, sex and PMI (no effect of sex or PMI).

TMEM97 is found in a higher proportion of synapses in AD

We recently described an increase of TMEM97 protein levels in biochemically isolated synaptic fractions from AD brain compared to controls *(40)*. In the present study, we were able to visualize the synaptic localization of TMEM97. The analysis of the 1,112,420 single synaptic terminals revealed an increased proportion of synapses with TMEM97 in AD when compared to healthy controls (fold increase: 1.77; β=3.65; p=0.004, **Fig. 2B**). In line with the hypothesis that TMEM97 is a binding partner of Aβ, we found that Aβ was present in postsynaptic terminals (**Fig. 2C**) and, importantly, that Aβ was found overlapping TMEM97 immunoreactivity at the same synapses (**Fig. 2D**).

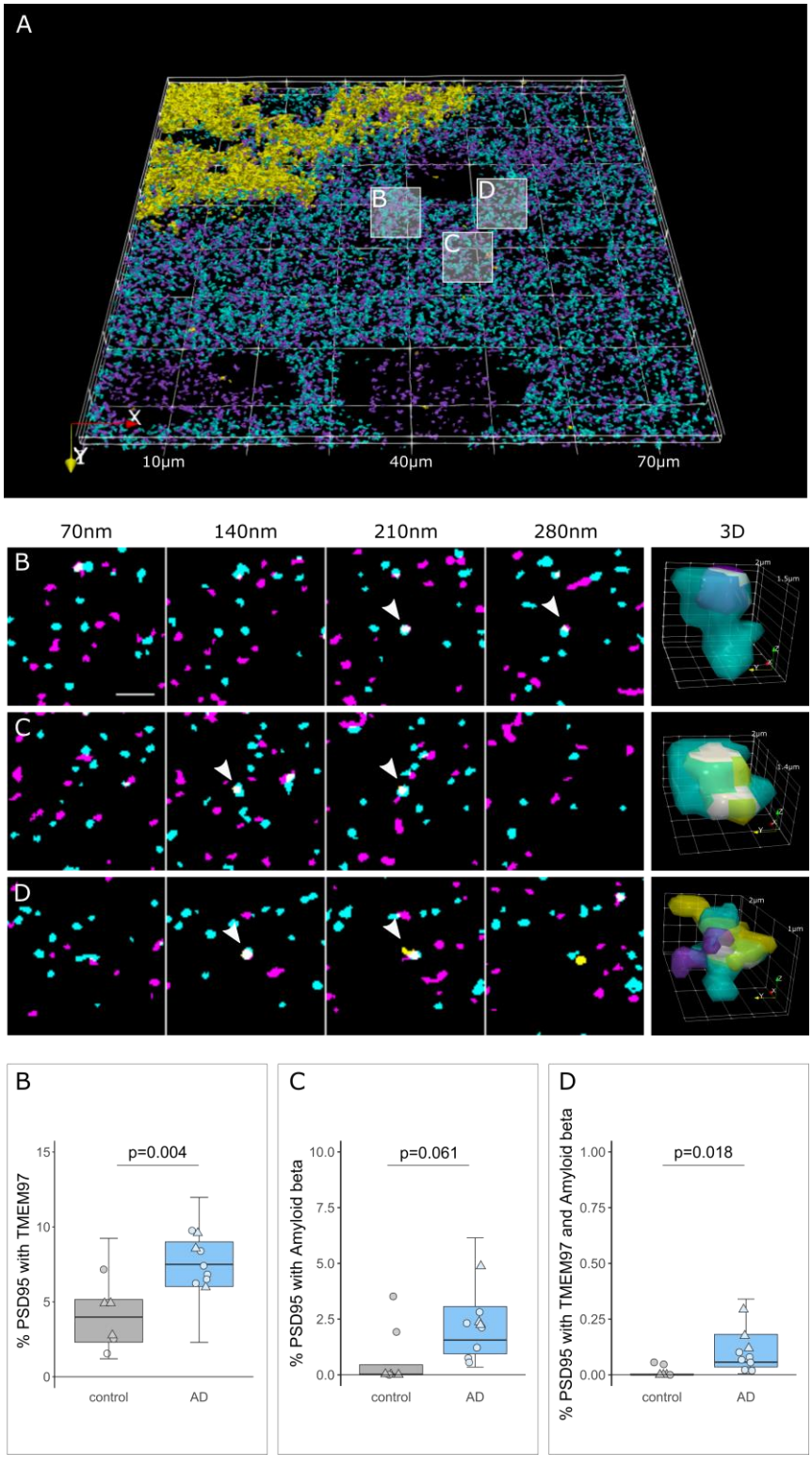

Fig. 2. TMEM97 is found at higher levels in AD synaptic terminals compared to healthy controls. 3D reconstructions were made from 20 consecutive 70nm-thick sections from a representative AD case stained for Aβ (yellow), TMEM97 (magenta) and PSD95 (cyan). In the top 3D reconstruction, white boxes label the magnified regions that highlight: a PSD95 terminal with TMEM97 (**B**), a postsynaptic terminal with Aβ (**C**) and a PSD95 synaptic terminal with both Aβ and TMEM97 (**D**). Below are shown four consecutive sections where the synaptic localization can be seen (arrowheads) and a 3D reconstruction of the pointed synapse where colocalization is highlighted in white. The plots below show the percent of postsynaptic terminals that contained TMEM97, Aβ, or both, in AD (blue) and control (grey) cases. Boxplots show quartiles and medians calculated from each image stack. Data points refer to case means (females, triangles; males, circles). Analysis was with linear mixed effects models including diagnostic group, sex and PMI (no effect of sex or PMI). Scale bar: 2µm.

In AD synapses TMEM97 and Aβ are close enough to generate a FRET signal

After confirming the presence of TMEM97 together with Aβ in synapses of AD cases, we next assessed the proximity of the immunoreactivity by FRET. In this single pixel analysis, those areas where the donor - Cy3 labelling Aβ - and the acceptor - Cy5 labelling TMEM97 - were found overlapping within a PSD95 positive object were quantified in the corrected donor excitation-acceptor emission image (**Fig. S1** and methods for further details). This quantification allowed us to detect FRET only when both donor and acceptor were present. To determine limitations of the technique, we measured the residual FRET signal in negative controls where only the donor or the acceptor was labelled and the maximum FRET signal was determined in the positive control where the donor and acceptor labelled the same target (**Fig. 3**, green bar of the plot shows the FRET signal between the negative and positive control levels).

In AD cases, we found that on average 38.4±9.66% of synaptic pixels where donor and acceptor were present, Aβ and TMEM97 were close enough to generate a FRET signal (**Fig. 3**, yellow boxplot). We also observe FRET between Aβ and PrP_c – which has also been observed to bind Aβ in model systems *(18)* and TMEM97 and PGRMC1 which are known to be binding partners in vitro and in human cases *(38)*. Further we see some FRET signal between Aβ and PSD95 which have been described to interact in some synapses, including in our previous study using a similar FRET approach in APP/PS1 mice *(7, 23, 24)* (**Fig. 3**).

To confirm that this effect was not occurring in all areas where donor and acceptor are present in the same pixel, we used a biological negative control looking for FRET between PSD95 and synaptophysin which are close but not interacting as they are separated by the synaptic cleft. As expected, there was not a significant FRET signal between these pre and postsynaptic proteins. There was also no FRET signal between PGRMC1 and PSD95 (**Fig. 3**). In summary, our FRET experiments confirm close proximity of Aβ and TMEM97, Aβ and PrP_c, TMEM97 and

PGRMC1, and Aβ and PSD95 which are robust as both technical and biological negative controls do not show FRET signal.

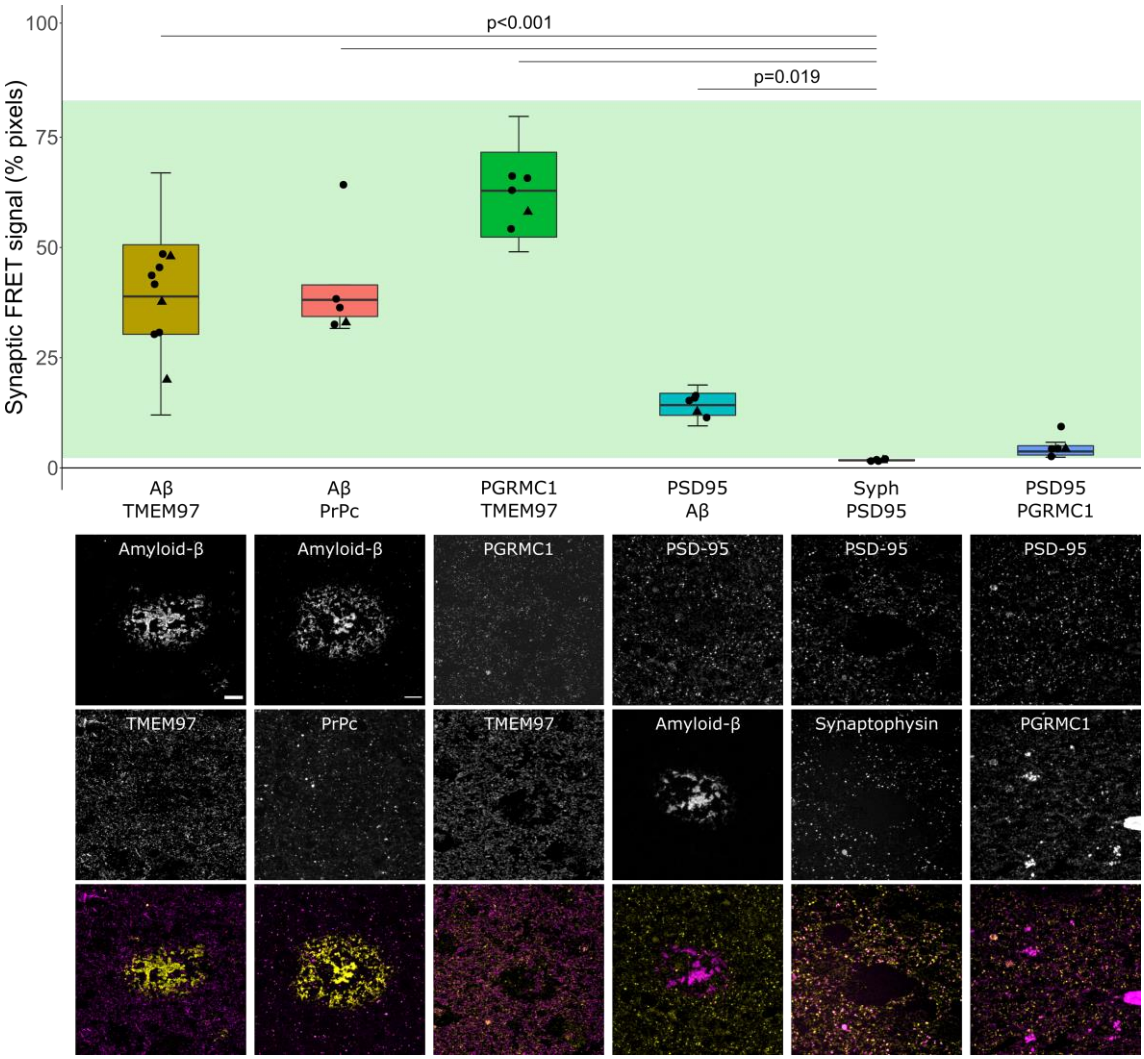

Fig. 3. **Aβ and TMEM97 are close enough at the AD synapses to generate a FRET effect.** The percent of synaptic pixels where FRET signal was detected by each protein pair are plotted. Green bar: mean of positive (top) and negative controls (bottom). Boxplots show quartiles and medians calculated from each image stack. Data points show case means (females, triangles; males, circles). Analysis with Tukey contrasts for multiple comparisons of means of the linear mixed effects models including assessed protein pair and sex (no effect of sex). Below the graph are shown maximum intensity projections of 10 consecutive 70nm-thick sections. The panel exhibits representative images of protein pairs tested for a FRET effect. Each targeted protein is shown individually in grayscale and in the merged images at the bottom, the donor is shown in yellow and the acceptor in magenta. Scale bar: 10µm. Abbreviations: PrP_c, cellular prion protein; Syph, synaptophysin.

TMEM97 antagonist reduces synaptic TMEM97-Aβ FRET signal in a mouse model of AD

Results from human brain observations suggested that TMEM97 may be a binding partner of Aβ. To determine whether this synaptic binding is reversible in vivo, we used the Sigma-

2/TMEM97 receptor complex allosteric antagonist CT1812 - currently in clinical trials for AD *(32, 33)* - in a recently described AD mouse model *(46)*. APP/PS1+Tau mice (APP-PS1+/- ; MAPT -/- ; CKTTA + ; Tg21221) and littermate controls were treated with either vehicle (n=10 APP/PS1+Tau, n=10 control) or the CT1812 compound (n=10 APP/PS1+Tau, n=10 control), which selectively binds to the Sigma-2 (TMEM97) receptor complex.

We first estimated the percent receptor occupancy of the compound, which was calculated based on the measured brain concentration of the drug (see methods and *(29)*). We observed a statistically significant sex difference in the percent of estimated receptor occupied by the drug. Male APP/PS1+Tau mice had an average of 85.13±6.4% estimated receptor occupancy, while females had an average of 69.69±11% (β=15.44; $p<0.001$, **Fig. 4B**). The increase in drug estimated receptor occupancy in male mice was observed in all genotypes (β=44.63; p=0.006, **Fig. S2C**). This difference could not be explained by any experimental procedures as all animals were given the same dose of compound from the same stock. The treatment of non-transgenic control mice did not affect the density of Aβ, Tau or PSD95 (**Fig. S2A-B**), confirming that treatment with this compound was not synaptotoxic.

Since it has been reported that only drug concentrations above 80% estimated receptor occupancy are effective *(29, 31)*, the effect on synaptic TMEM97 and Aβ localization was studied on the mice that reached that condition (n=5 APP/PS1+Tau mice, **Table S1**). CT1812 did not influence the overall densities of Aβ, TMEM97 or PSD95 nor the synaptic localization of Aβ and/or TMEM97 (**Fig. 4A, C, E**). When we modelled the effect of treatment and sex on the synaptic FRET signal between Aβ and TMEM97, we did not observe a difference between groups (vehicle mean 52.8±12%; treated mean 44.2±5.61%, **Fig. 4D**). However, the increase of estimated receptor occupancy by the drug correlated with a decrease of synaptic FRET signal between Aβ and TMEM97 (rho=-0.94, p=0.017, **Fig. 4F**).

Taken together, we found that in the CT1812 treated APP/PS1+Tau mice with estimated receptor occupancy in the therapeutic range, there was a decreased synaptic FRET signal between Aβ and TMEM97, indicating increased distance between the two proteins.

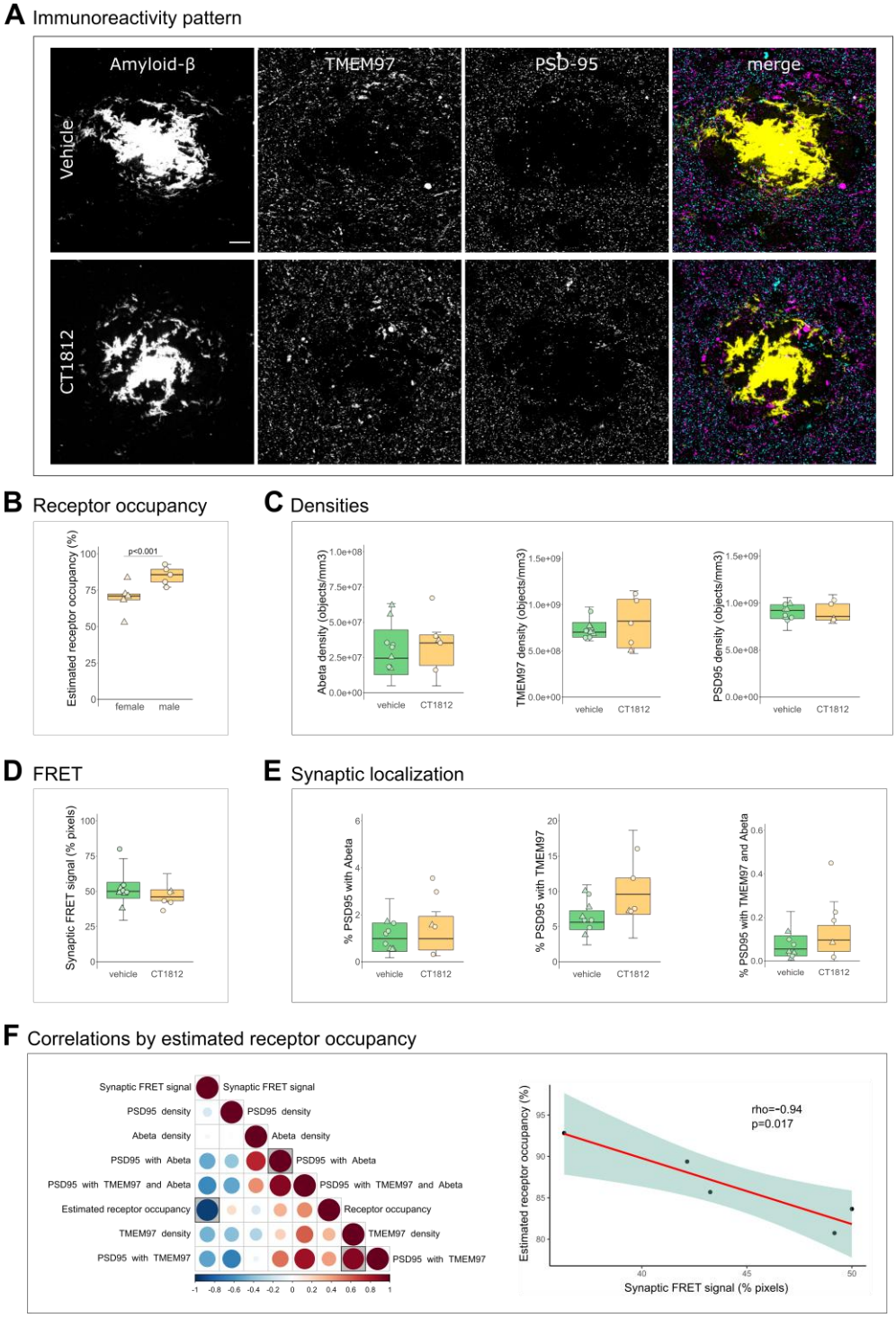

Fig. 4. **Effect of TMEM97 antagonist on synaptic Aβ and TMEM97 in the APP/PS1+Tau mice model.** Representative images of immunoreactivity patterns found in vehicle or CT1812 treated mice are shown in **A**. Images show maximum intensity projections of 16 consecutive 70nm-thick sections of cases stained for Aβ (yellow), TMEM97 (magenta) and PSD95 (cyan). **B**, the estimated percent of receptor occupancy by the drug in the CT1812 treated group. **D**, the percent of synaptic pixels that contain both Aβ and TMEM97, and FRET signal. **C,** quantification of overall densities of the three studied proteins. **D**, the postsynaptic terminals localisation of Aβ, TMEM97, or both. **F**, Correlations were estimated between measured parameters and a correlation matrix of the assessed variables is shown (left panel) in which the colour and size reflect the rho (scale below the plot) and the statistically significant correlations are highlighted with a shaded square. The correlation between percent estimated receptor occupancy and percent of synaptic FRET signal (right panel) displaying the regression line (red), the 95% confidence interval (green) and the Spearman correlation results (rho, p value). Scale bar: 10µm. Boxplots show quartiles and medians

calculated from each image stack. Data points refer to case means (females, triangles; males, circles). Analysis with linear mixed effects models including treatment group and sex interaction.

Discussion

In the present study, we visualized TMEM97 within individual postsynapses in human brain. In AD brain, TMEM97 levels were increased and in synapses, and TMEM97 was found in close enough proximity to Aβ to be binding.

TMEM97 (Sigma-2) has been previously linked to AD. In cellular models, it has been described that either by treatment with antagonists or by knocking out TMEM97 the internalization of Aβ is reduced *(31, 39)*. In an AD animal model, TMEM97 antagonists improved cognitive deficits *(29, 30)*. In human cases, TMEM97 has been found increased in biochemically isolated synapses of AD patients using an unbiased proteomic approach *(40)*. Those findings and the fact that TMEM97 antagonists are pharmacologically well studied, have brought the use of TMEM97 antagonists into Phase II clinical trials for AD treatment *(32, 33)*.

However, the relationship between Aβ and TMEM97 in human cases was not previously clear. Our current results support a mechanistic explanation that includes a direct interaction between Aβ and TMEM97, as suggested by the FRET findings (**Fig. 5**). Importantly, we found that this potential interaction may occur at the synapses, believed to be the earliest affected structure in the context of AD and the best pathological correlate of the characteristic cognitive decline *(1–3)*. Taken together, these findings link a therapeutic target (TMEM97) with a suspected pathological peptide (Aβ) in a key cellular structure (the synapse).

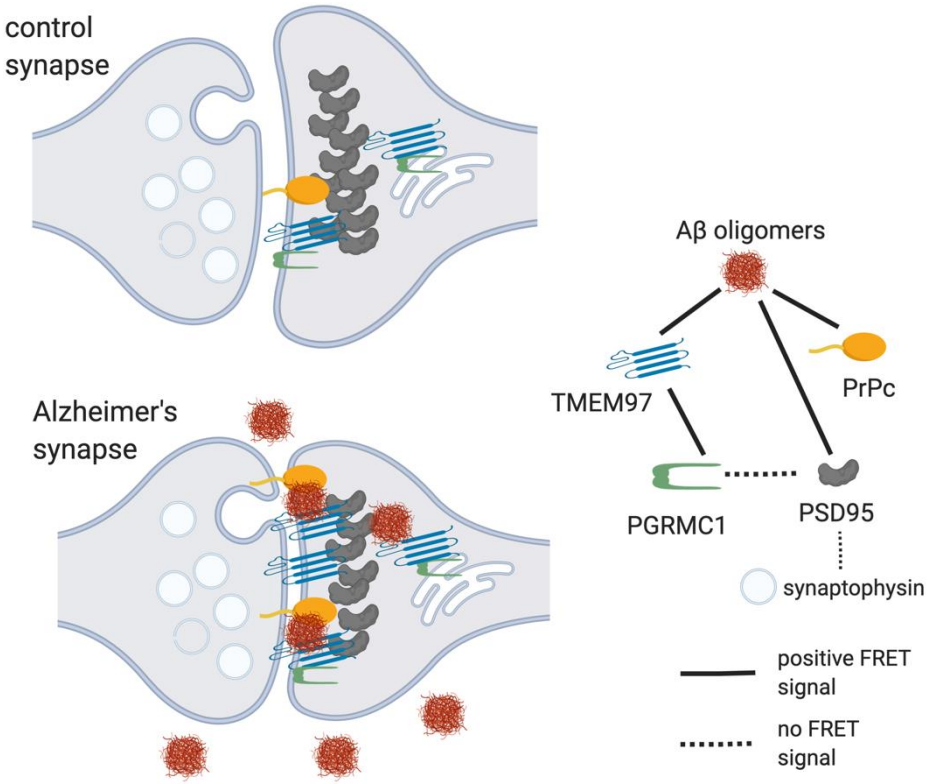

Fig. 5. Model of synaptic interactions of Aβ. Based on our study, we observe that Aβ is in close proximity to TMEM97, PSD95, and PrPc. Also, TMEM97 and PGRMC1 were found close enough to generate FRET signal. There was no FRET signal generated between PGRMC1 and PSD95 nor between PSD95 and synaptophysin which should not be in close enough proximity to generate a signal. These data are consistent with Aβ being a binding partner of these synaptic proteins either at the synaptic membrane or potentially within the post-synapse at spine apparatus.

The relationship between Aβ and synapses has been widely studied *(47)*. It has been shown that Aβ can be found in synapses of AD cases *(5, 46, 48)*, but the mechanisms by which Aβ induces synaptic toxicity remain unclear. The study of synaptic binding partners of Aβ yielded many candidates - reviewed in *(14–16)* . The most studied binding partner is the cellular prion protein (PrP_c), which through a cascade involving a complex with mGluR5 may lead to toxicity independently or via tau *(17–20)*. Other binding partners that have been suggested to bind Aβ include the α7-nicotinic receptor *(21)*, Ephrin A4 (EphA4) *(22)*, PSD95 *(7, 23, 24)* or LilrB2 *(25)*. It is likely that Aβ is in fact interacting with more than one protein *(18)*. Due its hydrophobic nature, Aβ binds to lipid membranes interrupting membrane fluidity and destabilizing several membrane receptors *(11)*. It is relevant to note that most binding partners have not been studied in human brain nor using human derived Aβ species *(11, 16)*. Further, while Aβ fibrils

bind non-specifically to a variety of surfaces, and Aβ monomers bind to several receptors when applied exogenously *(13)*, Aβ oligomers have been shown to bind saturably to a single site *(18, 29)* suggesting specific pharmacological interactions with receptors. Therefore, it has been tricky to determine which Aβ binding partners are relevant in living human brain. The structural state of Aβ (monomer, oligomer or fibril) recognized in the present array tomography studies is not clear, which is a limitation of the study, but within the limitations of the technique, we are able to observe proximity of synaptic proteins to a degree that has not previously been possible within human synapses. We observe that in human cases, TMEM97 and Aβ are close enough to generate a FRET effect, an observation that allows us to define close proximity, but does not conclusively show a direct interaction. The fact that we also found a FRET effect between Aβ and PrP_c in the same cases is in line with previous observations *(17, 18)* and reinforces the idea of multiple synaptic binding partners of Aβ at the synapses of AD cases.

How this interaction may be leading to synaptic dysfunction and subsequent neurodegeneration is less clear. Several mechanisms have been proposed linking Aβ and synaptic dysfunction involving excitatory imbalance *(4, 11)*. The fact that we found increased levels of TMEM97 in human AD cases and a close proximity between TMEM97 and Aβ at the synapses led us hypothesise that TMEM97 may be involved in the pathogenesis of AD and synaptic dysfunction. If so, the treatment with Sigma-2 receptor antagonists may result in an improvement of AD symptomatology, as has been previously described in an AD mouse model *(29)*. In the AD mouse model included in this study we were able to see a reduction of the Aβ potential binding to TMEM97 - as reflected by the decrease of FRET signal - in relation with increased estimated receptor occupancy of the drug. However, only five treated mice exhibited drug concentrations above the 80% estimated receptor occupancy, the drug concentration threshold previously defined as effective *(29)*. The reduced number of mice with high levels of drug make us cautious about the correlation found while highlight an unexpected finding: a statistically significant

increase in drug concentration in male when compared with female mice. None of the variables controlled in the present study could explain the drug concentration differences between males and females and therefore we hypothesise that sex-related biological differences may be underlying the drug metabolism or blood brain barrier penetration. This finding is consistent with unpublished data on sex-related differences in drug exposure of CT1812 in rodents that is not observed in other non-rodent species or in human clinical trial subjects (unpublished data). This is the first study in which CT81812 has been administered to animal models in food, however human clinical trials suggest no difference in CT1812 pharmacokinetics in a fed or fasted state *(33)*. It is important to note that Izzo and colleagues found an improvement of cognition in mice exhibiting more than 80% estimated receptor occupancy, something only seen in one female of our study *(29)*. Further, Izzo and colleagues included only male mice in the study, and therefore the present findings on female mice should be taken into consideration to ensure the efficacy of treatments in future studies. These findings may be in line with the increasing body of literature describing sex differences in mice models of AD that may be translated to human cases *(49–51)*.

Although we could see a reduction in the synaptic FRET signal of Aβ with TMEM97 in the >80% estimated receptor occupancy group, and a significant correlation with drug brain concentration in the treated group, the treatment of the AD mouse model with TMEM97 antagonists did not result in a recovery of synaptic densities nor a decrease of Aβ synaptic localization. CT1812 has been previously demonstrated to selectively displace Aβ oligomers, but not monomer from synaptic receptor sites and facilitate its clearance out of the brain *(52)*, suggesting that the Aβ that is interacting with TMEM97 observed in this study may be predominantly fibrils. However, disrupting this interaction may be sufficient to improve synaptic function which could explain the behavioural recovery seen in previous mouse studies with CT1812 treatment *(29)*. Alternatively, the 28 day treatment period used here may not have been sufficiently long to

observe a change in synaptic density; previous studies demonstrating CT1812-mediated improvement in cognitive performance were conducted following 9-10 weeks of administration *(52)*.

A previously published model of CT1812's mechanism of action proposes that the sigma-2 receptor complex regulates other Aβ oligomer receptors (composed of LilRB2, NGR and PrPc), and when CT1812 binds to TMEM97, allosteric interactions between the sigma-2 receptor and the oligomer receptor change the oligomer receptors' shape, destabilize the binding pocket, and increase the off-rate of Aβ oligomers from their receptor. Therefore CT1812 does not compete directly with oligomers at the same site *(52)*. In tumor cells, the canonical sigma-2 ligand DTG binds to sigma-2 receptors at a location on the TMEM97 protein *(26)*, and CT1812 displaces radiolabeled DTG binding, but the precise binding location of CT1812 has not been directly determined. Our data indicate that TMEM97 and Aβ are in close proximity where they could be binding, but we cannot rule out that Aβ may be binding to other nearby proteins instead of directly interacting with TMEM97.

Regarding the mechanism by which TMEM97-Aβ interaction may be linked to synaptic dysfunction, several studies suggest a role of TMEM97 in calcium homeostasis *(30, 36, 37)*, which is critical for the above mentioned excitatory imbalance that regulates learning and memory, however, CT1812 has not been shown to cause alterations in calcium homeostasis. Also in line with the hypothesis of Aβ binding to lipid membranes *(11)*, TMEM97 is thought to be a endo-lysosome-related protein essential for the internalization of cholesterol molecules like LDL through the formation of a complex with PGRMC1 which has itself been linked to cellular toxicity *(38, 53)*. This work indicates that future studies are warranted to explore sex differences and the displacement of Aβ species towards other receptors, bringing potential multi-target and sex-specific approaches for the treatment of AD.

In summary, in human AD brains we found increased synaptic levels of TMEM97 and close colocalization of TMEM97 with Aβ in synapses. This supports the idea that TMEM97 is a synaptic binding partner for Aβ, which is important as this interaction can be modulated by drugs.

Materials and Methods

Study design

The aim of the study was to investigate the synaptic localization of TMEM97 and its proximity to Aβ in post mortem human brain tissue. We combined array tomography and FRET microscopy to increase the axial and lateral resolution, respectively. Besides technical controls, other relevant proteins previously described to interact or not interact were also included as biological controls. Human cases selection was based on clinicopathological diagnoses as internationally recommended and the number of cases was defined by tissue availability and previous studies experience. Controls and AD cases were age matched, and beside this parameters no other exclusion criteria where applied.

The same microscopy approach was used to study the effect of modulating the potential TMEM97- Aβ interaction in an APP/PS1+Tau mice model by treating them with CT1812 Sigma-2 receptor complex allosteric antagonist or vehicle. Groups were balanced for male and female mice. While all mice were analysed, a sub-analysis was performed following the inclusion criteria of >80% receptor occupancy by the drug, as a recommended therapeutic window *(29)*.
The units plotted are always individual cases (human or mice) that represent the mean of four 70nm thick consecutive sections ribbons from two adjacent tissue blocks from the same brain region.

The immunostaining, image acquisition, image processing and analyses were performed blinded to the clinicopathological diagnosis. Bias was also minimized by setting the same parameters for image acquisition and image analysis for all the included cases.

Human cases

Patients fulfilling clinical and neuropathological criteria for Alzheimer's disease (n = 9) *(54)*, or cognitively healthy control cases (n = 6) were included in this study. Clinical and neuropathological data were retrospectively obtained from the clinical charts available at the Edinburgh Brain Bank. Neuropathological stages were applied according to international recommendations *(54–56)*. Details of the human cases included are found in **Table 1**. Use of human tissue for postmortem studies has been reviewed and approved by the Edinburgh Brain Bank ethics committee and the ACCORD medical research ethics committee, AMREC (ACCORD is the Academic and Clinical Central Office for Research and Development, a joint office of the University of Edinburgh and NHS Lothian, approval number 15-HV-016). The Edinburgh Brain Bank is a Medical Research Council funded facility with research ethics committee (REC) approval (16/ES/0084).

Mice

Mice expressing both human tau and the APP/PS1 transgene (APP/PS1+Tau) were generated as previously described *(46)*. Briefly, two feeder lines were bred to produce experimental genotypes. The feeder lines were line 1: mice heterozygous for an APP/PS1 transgene and a CK-tTA driver transgene and homozygous for knockout of endogenous mouse tau mouse tau; line 2: heterozygous for the Tg21221 human wild type tau transgene driven by CK-tTA and homozygous for knockout of endogenous mouse tau mouse tau *(46)*. APP/PS1+Tau mice (n=20) and littermate control mice not expressing APP/PS1 nor tau (n=20) were aged to 9 months old before starting CT1812 treatment. Mice of both sexes were randomised into vehicle or control groups. Animal experiments were conducted in compliance with national and institutional guidelines including the Animals [Scientific Procedures Act] 1986 (UK), and the Council Directive 2010/63EU of the European Parliament and the Council of 22 September 2010 on the protection of animals used for scientific purposes, and had full Home Office ethical approval.

Mice were singly housed and habituated with double concentration Hartley's strawberry jelly 4 days prior to the start of the experiment. CT1812 fumarate was dissolved in DMSO and added to cold jelly solution to make up the final volume of 0.6mg/ml concentration before being allowed to set. Each week, a batch of Hartley's strawberry jelly containing CT1812 or vehicle (plain triple strength jelly) was made. Mice were weighed at the beginning of each week to determine the weight of jelly to be given for that week, and were dosed daily for one month with jelly containing vehicle or CT1812 10 mg/kg/day.

After 28 days of treatment, mice were sacrificed by terminal anaesthesia. Blood was collected for drug levels then mice were perfused with phosphate buffered saline (0.1M). Brains were removed and the cerebellum snap frozen for testing drug levels. One cerebral hemisphere (selected randomly) was drop fixed in 4% paraformaldehyde. The other hemisphere was dissected and entorhinal cortex processed for array tomography. The rest of the hemisphere was snap frozen for biochemical studies.

Estimated percent receptor occupancy was calculated according to the formula (concentration/Ki)/[(concentration/Ki) + 1)], where Ki is determined by radioligand competition binding *(29)*.

The main study combining array tomography and FRET experiments were performed on APP/PS1+tau mice (n=10) and control littermates of mice (n=8). Details are found in **Table S1**. Standard array tomography imaging (without FRET) was performed on APP/PS1+tau mice (n=9) and control littermates of mice (n=13) to test whether there were any drug effects on synapse density.

Array tomography tissue processing

Fresh brain tissue samples from human and mouse cases were collected and processed as previously described *(44)*. Briefly, small pieces of brain tissue comprising all cortical layers were fixed in 4% paraformaldehyde and 2.5% sucrose in 20mM phosphate-buffered saline pH 7.4

(PBS) for up to 3h. Samples were then dehydrated through ascending concentrations of cold ethanol until embedding into LR White resin (Electron Microscopy Sciences, EMS), which was allowed to polymerize overnight at >50°C. Tissue blocks were then stored at room temperature until used. For each case, two blocks corresponding to BA20/21 for human cases, or one from entorhinal cortex for mouse samples, were cut into 70nm thick sections using an ultramicrotome (Leica) equipped with a Jumbo Histo Diamond Knife (Diatome, Hatfield, PA). Ribbons of at least 20 consecutive sections were collected in gelatine subbed coverslips.

Immunofluorescence

70nm thick ribbons were immuno-labelled as described previously *(44)*. Briefly, coverslips were first incubated with Tris-glycine solution 5min at room temperature followed by blocking of non-specific antigens with a cold water fish blocking buffer (Sigma-Aldrich) for 30min. Samples were then incubated for 2h with primary antibodies, washed with Tris-buffered saline (TBS) solution and secondary antibodies applied for 30min. After another TBS washing cycle, coverslips were mounted on microscope slides with Immu-Mount (Fisher Scientific) mounting media. For the detailed information of the primary and secondary antibodies used, please see **Table S2**.

Image acquisition

For FRET imaging, images of the same field of view of the consecutive sections were acquired using a Leica TCS8 confocal with 63x 1.4 NA oil objective. Alexa fluor 488, Cy3 or Cy5 were sequentially excited with the 488, 552 or 638 laser lines and imaged in 500 to 550 nm, 570 to 634 nm or 649 to 710 nm spectral windows, respectively. For FRET analysis, the spectral window of the Cy5 (the acceptor, 649 to 710 nm) was also imaged under the excitation of Cy3 (the donor, 552 nm). This setting allowed us to record the transfer of energy from donor molecules to acceptors based on intensity (sensitized emission FRET, *(43, 45)*, **Fig. S1**). Laser and detector

settings were maintained through the whole study avoiding major saturation, which is only applied in figures for image visualization purposes.

Standard array tomography imaging (without FRET) was performed on APP/PS1+tau mice (n=9) and control littermates of mice (n=13) to test whether there were any drug effects on synapse density. These images were acquired on a Ziess Axio Imager Z2 epifluorescence microscope with a 63x 1.4 NA oil immersion objective and a CoolSNAP digital camera.

Image processing and analysis

Images from consecutive sections were transformed into stacks using ImageJ *(57, 58)*. The following steps were performed using an in-house algorithm developed for array tomography image processing and analysis freely available (based on *(59)*, available at *add upon acceptance for publication*, **Fig. S1**). The consecutive images were first aligned using a rigid and affine registration. For the study of the immunoreactivity patterns, semi-automatic local threshold based on mean values was applied specifically for each channel yet common for all the included images. Importantly, only those objects detected in more than one consecutive section (3D objects) were quantified, allowing us to reduce non-specific signals. The number of objects from each channel were quantified and neuropil concentration in mm^3 of tissue established after removing confounding structures (i.e. blood vessels or cell bodies). In order to investigate the relationship between channels, colocalization was based on a minimum overlap of 10% of the area of the synaptic terminals. Finally, in AD cases, the concentration of objects in each channel or the colocalizing objects were also determined by calculating the Euclidean distance between the centroid of each object and the closest point to the plaque core perimeter. Objects were then binned in 10μm groups.

For FRET analysis, donor-only (Cy3) and acceptor-only (Cy5) samples were imaged in each imaging session in order to calculate the donor emission crosstalk with the acceptor emission (beta parameter) and the direct excitation of the acceptor by the donor excitation laser line

(gamma parameter) *(43, 60)*. Aligned stacks of images corresponding to the acceptor emission under donor excitation line (FRET image) were first corrected for the above-mentioned parameters. Each pixel of the FRET image was corrected according to the pixel intensity of either donor-excited donor-emission images or acceptor-excited acceptor-emission images **Fig. S1**). Using the binary masks created before corresponding to postsynaptic terminals, donor and acceptor images, the pixels where the three objects were found overlapping were studied. The percent of pixels where any FRET signal was observed were quantified, allowing us to have a qualitative measure of the occurrence of the FRET effect.

Statistics

Brain weight, age at death, and PMI differences between groups were analysed with t-test or Wilcoxon test depending on the Shapiro-Wilk Normality test results. Sex and *APOE* genotype were analysed with Fisher-exact test. The comparison between groups in all the other studied variables was analysed using linear mixed models including sex and PMI as covariates and case as a random effect to account for multiple measures per case. All the analyses were performed with R *(61)* and the scripts and full statistical results can be found at *add upon acceptance for publication*.

Data sharing

Protocols, image analysis scripts and R scripts for statistical analysis are available at *link to be added upon acceptance for publication*. Raw images available from the corresponding author upon reasonable request.

Supplementary materials

Table S1. Mice included in array tomography-FRET experiments.

Table S2. Antibodies.

Fig. S1. Image analysis pipeline.

Fig. S2. Effect of sigma-2 receptor antagonist on PSD95, Aβ and tau in the non-transgenic control mice and APP/PS1+Tau mice.

References

1. S. T. DeKosky, S. W. Scheff, Synapse loss in frontal cortex biopsies in Alzheimer's disease: correlation with cognitive severity, *Ann. Neurol.* **27**, 457–464 (1990).

2. S. W. Scheff, D. A. Price, F. A. Schmitt, E. J. Mufson, Hippocampal synaptic loss in early Alzheimer's disease and mild cognitive impairment, *Neurobiol. Aging* **27**, 1372–1384 (2006).

3. R. D. Terry, E. Masliah, D. P. Salmon, N. Butters, R. DeTeresa, R. Hill, L. A. Hansen, R. Katzman, Physical basis of cognitive alterations in alzheimer's disease: Synapse loss is the major correlate of cognitive impairment, *Ann. Neurol.* **30**, 572–580 (1991).

4. Y. Chen, A. K. Y. Fu, N. Y. Ip, Synaptic dysfunction in Alzheimer's disease: Mechanisms and therapeutic strategies, *Pharmacol. Ther.* **195**, 186–198 (2019).

5. R. M. Koffie, T. Hashimoto, H.-C. Tai, K. R. Kay, A. Serrano-Pozo, D. Joyner, S. Hou, K. J. Kopeikina, M. P. Frosch, V. M. Lee, D. M. Holtzman, B. T. Hyman, T. L. Spires-Jones, Apolipoprotein E4 effects in Alzheimer's disease are mediated by synaptotoxic oligomeric amyloid-β, *Brain J. Neurol.* **135**, 2155–2168 (2012).

6. L. F. Lue, Y. M. Kuo, A. E. Roher, L. Brachova, Y. Shen, L. Sue, T. Beach, J. H. Kurth, R. E. Rydel, J. Rogers, Soluble amyloid beta peptide concentration as a predictor of synaptic change in Alzheimer's disease, *Am. J. Pathol.* **155**, 853–862 (1999).

7. E. K. Pickett, R. M. Koffie, S. Wegmann, C. M. Henstridge, A. G. Herrmann, M. Colom-Cadena, A. Lleo, K. R. Kay, M. Vaught, R. Soberman, D. M. Walsh, B. T. Hyman, T. L. Spires-Jones, Non-Fibrillar Oligomeric Amyloid-β within Synapses, *J. Alzheimers Dis. JAD* **53**, 787–800 (2016).

8. G. M. Shankar, S. Li, T. H. Mehta, A. Garcia-Munoz, N. E. Shepardson, I. Smith, F. M. Brett, M. A. Farrell, M. J. Rowan, C. A. Lemere, C. M. Regan, D. M. Walsh, B. L. Sabatini, D. J. Selkoe, Amyloid-beta protein dimers isolated directly from Alzheimer's brains impair synaptic plasticity and memory, *Nat. Med.* **14**, 837–842 (2008).

9. T. L. Spires-Jones, B. T. Hyman, The intersection of amyloid beta and tau at synapses in Alzheimer's disease, *Neuron* **82**, 756–771 (2014).

10. C. M. Henstridge, B. T. Hyman, T. L. Spires-Jones, Beyond the neuron–cellular interactions early in Alzheimer disease pathogenesis, *Nat. Rev. Neurosci.* **20**, 94–108 (2019).

11. S. Li, D. J. Selkoe, A mechanistic hypothesis for the impairment of synaptic plasticity by soluble Aβ oligomers from Alzheimer's brain, *J. Neurochem.* **154**, 583–597 (2020).

12. M. Colom-Cadena, T. Spires-Jones, H. Zetterberg, K. Blennow, A. Caggiano, S. T. DeKosky, H. Fillit, J. E. Harrison, L. S. Schneider, P. Scheltens, W. de Haan, M. Grundman, C. H. van Dyck, N. J. Izzo, S. M. Catalano, Synaptic Health Endpoints Working Group, The clinical promise of biomarkers of synapse damage or loss in Alzheimer's disease, *Alzheimers Res. Ther.* **12**, 21 (2020).

13. I. Benilova, B. De Strooper, Promiscuous Alzheimer's amyloid: yet another partner, *Science* **341**, 1354–1355 (2013).

14. H. H. Jarosz-Griffiths, E. Noble, J. V. Rushworth, N. M. Hooper, Amyloid-β Receptors: The Good, the Bad, and the Prion Protein, *J. Biol. Chem.* **291**, 3174–3183 (2016).

15. B. Mroczko, M. Groblewska, A. Litman-Zawadzka, J. Kornhuber, P. Lewczuk, Cellular Receptors of Amyloid β Oligomers (AβOs) in Alzheimer's Disease, *Int. J. Mol. Sci.* **19**, 1884 (2018).

16. L. M. Smith, S. M. Strittmatter, Binding Sites for Amyloid-β Oligomers and Synaptic Toxicity, *Cold Spring Harb. Perspect. Med.* **7**, a024075 (2017).

17. J. Laurén, D. A. Gimbel, H. B. Nygaard, J. W. Gilbert, S. M. Strittmatter, Cellular prion protein mediates impairment of synaptic plasticity by amyloid-β oligomers, *Nature* **457**, 1128–1132 (2009).

18. L. M. Smith, M. A. Kostylev, S. Lee, S. M. Strittmatter, Systematic and standardized comparison of reported amyloid-β receptors for sufficiency, affinity, and Alzheimer's disease relevance, *J. Biol. Chem.* **294**, 6042–6053 (2019).

19. J. W. Um, A. C. Kaufman, M. Kostylev, J. K. Heiss, M. Stagi, H. Takahashi, M. E. Kerrisk, A. Vortmeyer, T. Wisniewski, A. J. Koleske, E. C. Gunther, H. B. Nygaard, S. M. Strittmatter, Metabotropic glutamate receptor 5 is a coreceptor for Alzheimer aβ oligomer bound to cellular prion protein, *Neuron* **79**, 887–902 (2013).

20. Y. Zhang, Y. Zhao, L. Zhang, W. Yu, Y. Wang, W. Chang, Cellular Prion Protein as a Receptor of Toxic Amyloid-β42 Oligomers Is Important for Alzheimer's Disease, *Front. Cell. Neurosci.* **13**, 339 (2019).

21. H. R. Parri, C. M. Hernandez, K. T. Dineley, Research update: Alpha7 nicotinic acetylcholine receptor mechanisms in Alzheimer's disease, *Biochem. Pharmacol.* **82**, 931–942 (2011).

22. L. M. Vargas, N. Leal, L. D. Estrada, A. González, F. Serrano, K. Araya, K. Gysling, N. C. Inestrosa, E. B. Pasquale, A. R. Alvarez, EphA4 Activation of c-Abl Mediates Synaptic Loss and LTP Blockade Caused by Amyloid-β Oligomers, *PLOS ONE* **9**, e92309 (2014).

23. P. N. Lacor, M. C. Buniel, L. Chang, S. J. Fernandez, Y. Gong, K. L. Viola, M. P. Lambert, P. T. Velasco, E. H. Bigio, C. E. Finch, G. A. Krafft, W. L. Klein, Synaptic targeting by Alzheimer's-related amyloid beta oligomers, *J. Neurosci. Off. J. Soc. Neurosci.* **24**, 10191–10200 (2004).

24. E. Pham, L. Crews, K. Ubhi, L. Hansen, A. Adame, A. Cartier, D. Salmon, D. Galasko, S. Michael, J. N. Savas, J. R. Yates, C. Glabe, E. Masliah, Progressive accumulation of amyloid-beta oligomers in Alzheimer's disease and in amyloid precursor protein transgenic mice is accompanied by selective alterations in synaptic scaffold proteins, *FEBS J.* **277**, 3051–3067 (2010).

25. T. Kim, G. S. Vidal, M. Djurisic, C. M. William, M. E. Birnbaum, K. C. Garcia, B. T. Hyman, C. J. Shatz, Human LilrB2 Is a β-Amyloid Receptor and Its Murine Homolog PirB Regulates Synaptic Plasticity in an Alzheimer's Model, *Science* **341**, 1399–1404 (2013).

26. A. Alon, H. R. Schmidt, M. D. Wood, J. J. Sahn, S. F. Martin, A. C. Kruse, Identification of the gene that codes for the σ2 receptor, *Proc. Natl. Acad. Sci. U. S. A.* **114**, 7160–7165 (2017).

27. L. Guo, X. Zhen, Sigma-2 receptor ligands: neurobiological effects, *Curr. Med. Chem.* **22**, 989–1003 (2015).

28. H. R. Schmidt, A. C. Kruse, The Molecular Function of σ Receptors: Past, Present, and Future, *Trends Pharmacol. Sci.* **40**, 636–654 (2019).

29. N. J. Izzo, A. Staniszewski, L. To, M. Fa, A. F. Teich, F. Saeed, H. Wostein, T. Walko, A. Vaswani, M. Wardius, Z. Syed, J. Ravenscroft, K. Mozzoni, C. Silky, C. Rehak, R. Yurko, P. Finn, G. Look, G. Rishton, H. Safferstein, M. Miller, C. Johanson, E. Stopa, M. Windisch, B. Hutter-Paier, M. Shamloo, O. Arancio, H. LeVine, S. M. Catalano, Alzheimer's therapeutics targeting amyloid beta 1-42 oligomers I: Abeta 42 oligomer binding to specific neuronal receptors is displaced by drug candidates that improve cognitive deficits, *PloS One* **9**, e111898 (2014).

30. B. Yi, J. J. Sahn, P. M. Ardestani, A. K. Evans, L. Scott, J. Z. Chan, S. Iyer, A. Crisp, G. Zuniga, J. Pierce-Shimomura, S. F. Martin, M. Shamloo, Small molecule modulator of sigma 2 receptor is neuroprotective and reduces cognitive deficits and neuro-inflammation in experimental models of Alzheimer's disease, *J. Neurochem.* **140**, 561–575 (2017).

31. N. J. Izzo, J. Xu, C. Zeng, M. J. Kirk, K. Mozzoni, C. Silky, C. Rehak, R. Yurko, G. Look, G. Rishton, H. Safferstein, C. Cruchaga, A. Goate, M. A. Cahill, O. Arancio, R. H. Mach, R. Craven, E. Head, H. L. Iii, T. L. Spires-Jones, S. M. Catalano, Alzheimer's Therapeutics Targeting Amyloid Beta 1–42 Oligomers II: Sigma-2/PGRMC1 Receptors Mediate Abeta 42 Oligomer Binding and Synaptotoxicity, *PLOS ONE* **9**, e111899 (2014).

32. Cognition Therapeutics, *A Randomized, Double-Blind, Placebo-Controlled, Parallel-Group, Phase 2 Study to Evaluate the Safety and Efficacy of CT1812 in Subjects With Mild to Moderate Alzheimer's Disease.* (clinicaltrials.gov, 2020; https://clinicaltrials.gov/ct2/show/NCT03507790).

33. M. Grundman, R. Morgan, J. D. Lickliter, L. S. Schneider, S. DeKosky, N. J. Izzo, R. Guttendorf, M. Higgin, J. Pribyl, K. Mozzoni, H. Safferstein, S. M. Catalano, A phase 1 clinical trial of the sigma-2 receptor complex allosteric antagonist CT1812, a novel therapeutic candidate for Alzheimer's disease, *Alzheimers Dement. N. Y. N* **5**, 20–26 (2019).

34. M. Murphy, M. J. Pykett, P. Harnish, K. D. Zang, D. L. George, Identification and characterization of genes differentially expressed in meningiomas, *Cell Growth Differ. Mol. Biol. J. Am. Assoc. Cancer Res.* **4**, 715–722 (1993).

35. C. Zeng, C.-C. Weng, M. E. Schneider, L. Puentes, A. Riad, K. Xu, M. Makvandi, L. Jin, W. G. Hawkins, R. H. Mach, TMEM97 and PGRMC1 do not mediate sigma-2 ligand-induced cell death, *Cell Death Discov.* **5**, 1–12 (2019).

36. G. Cassano, G. Gasparre, M. Niso, M. Contino, V. Scalera, N. A. Colabufo, F281, synthetic agonist of the sigma-2 receptor, induces Ca2+ efflux from the endoplasmic reticulum and mitochondria in SK-N-SH cells, *Cell Calcium* **45**, 340–345 (2009).

37. B. J. Vilner, W. D. Bowen, Modulation of Cellular Calcium by Sigma-2 Receptors: Release from Intracellular Stores in Human SK-N-SH Neuroblastoma Cells, *J. Pharmacol. Exp. Ther.* **292**, 900–911 (2000).

38. A. Riad, C. Zeng, C.-C. Weng, H. Winters, K. Xu, M. Makvandi, T. Metz, S. Carlin, R. H. Mach, Sigma-2 Receptor/TMEM97 and PGRMC-1 Increase the Rate of Internalization of LDL by LDL Receptor through the Formation of a Ternary Complex, *Sci. Rep.* **8**, 16845 (2018).

39. A. Riad, Z. Lengyel-Zhand, C. Zeng, C.-C. Weng, V. M.-Y. Lee, J. Q. Trojanowski, R. H. Mach, The Sigma-2 Receptor/TMEM97, PGRMC1, and LDL Receptor Complex Are Responsible for the Cellular Uptake of Aβ42 and Its Protein Aggregates, *Mol. Neurobiol.* **57**, 3803–3813 (2020).

40. R. Hesse, M. L. Hurtado, R. J. Jackson, S. L. Eaton, A. G. Herrmann, M. Colom-Cadena, M. Tzioras, D. King, J. Rose, J. Tulloch, C.-A. McKenzie, C. Smith, C. M. Henstridge, D. Lamont, T. M. Wishart, T. L. Spires-Jones, Comparative profiling of the synaptic proteome from Alzheimer's disease patients with focus on the APOE genotype, *Acta Neuropathol. Commun.* **7**, 214 (2019).

41. K. D. Micheva, S. J. Smith, Array tomography: a new tool for imaging the molecular architecture and ultrastructure of neural circuits, *Neuron* **55**, 25–36 (2007).

42. T. Förster, Delocalization excitation and excitation transfer, *Mod. Quantum Chem.* (1965) (available at https://ci.nii.ac.jp/naid/10021068765/).

43. T. Zimmermann, Photobleaching and Sensitized Emission-Based Methods for the Detection of Förster Resonance Energy Transfer, *Methods Mol. Biol. Clifton NJ* **2040**, 235–274 (2019).

44. K. R. Kay, C. Smith, A. K. Wright, A. Serrano-Pozo, A. M. Pooler, R. Koffie, M. E. Bastin, T. H. Bak, S. Abrahams, K. J. Kopeikina, D. McGuone, M. P. Frosch, T. H. Gillingwater, B. T. Hyman, T. L. Spires-Jones, Studying synapses in human brain with array tomography and electron microscopy, *Nat. Protoc.* **8**, 1366–1380 (2013).

45. B. Hellenkamp, S. Schmid, O. Doroshenko, O. Opanasyuk, R. Kühnemuth, S. Rezaei Adariani, B. Ambrose, M. Aznauryan, A. Barth, V. Birkedal, M. E. Bowen, H. Chen, T. Cordes, T. Eilert, C. Fijen, C. Gebhardt, M. Götz, G. Gouridis, E. Gratton, T. Ha, P. Hao, C. A. Hanke, A. Hartmann, J. Hendrix, L. L. Hildebrandt, V. Hirschfeld, J. Hohlbein, B. Hua, C. G. Hübner, E. Kallis, A. N. Kapanidis, J.-Y. Kim, G. Krainer, D. C. Lamb, N. K. Lee, E. A. Lemke, B. Levesque, M. Levitus, J. J. McCann, N. Naredi-Rainer, D. Nettels, T. Ngo, R. Qiu, N. C. Robb, C. Röcker, H. Sanabria, M. Schlierf, T. Schröder, B. Schuler, H. Seidel, L. Streit, J. Thurn, P. Tinnefeld, S. Tyagi, N. Vandenberk, A. M. Vera, K. R. Weninger, B. Wünsch, I. S. Yanez-Orozco, J. Michaelis, C. A. M. Seidel, T. D. Craggs, T. Hugel, Precision and accuracy of single-molecule FRET measurements-a multi-laboratory benchmark study, *Nat. Methods* **15**, 669–676 (2018).

46. E. K. Pickett, A. G. Herrmann, J. McQueen, K. Abt, O. Dando, J. Tulloch, P. Jain, S. Dunnett, S. Sohrabi, M. P. Fjeldstad, W. Calkin, L. Murison, R. J. Jackson, M. Tzioras, A. Stevenson, M. d'Orange, M. Hooley, C. Davies, M. Colom-Cadena, A. Anton-Fernandez, D. King, I. Oren, J.

Rose, C.-A. McKenzie, E. Allison, C. Smith, O. Hardt, C. M. Henstridge, G. E. Hardingham, T. L. Spires-Jones, Amyloid Beta and Tau Cooperate to Cause Reversible Behavioral and Transcriptional Deficits in a Model of Alzheimer's Disease, *Cell Rep.* **29**, 3592-3604.e5 (2019).

47. S. Forner, D. Baglietto-Vargas, A. C. Martini, L. Trujillo-Estrada, F. M. LaFerla, Synaptic Impairment in Alzheimer's Disease: A Dysregulated Symphony, *Trends Neurosci.* **40**, 347–357 (2017).

48. T. Bilousova, C. A. Miller, W. W. Poon, H. V. Vinters, M. Corrada, C. Kawas, E. Y. Hayden, D. B. Teplow, C. Glabe, R. Albay, G. M. Cole, E. Teng, K. H. Gylys, Synaptic Amyloid-β Oligomers Precede p-Tau and Differentiate High Pathology Control Cases, *Am. J. Pathol.* **186**, 185–198 (2016).

49. K. S. Abd-Elrahman, A. Albaker, J. M. de Souza, F. M. Ribeiro, M. G. Schlossmacher, M. Tiberi, A. Hamilton, S. S. G. Ferguson, Aβ oligomers induce pathophysiological mGluR5 signaling in Alzheimer's disease model mice in a sex-selective manner, *Sci. Signal.* **13** (2020), doi:10.1126/scisignal.abd2494.

50. E. J. Davis, L. Broestl, S. Abdulai-Saiku, K. Worden, L. W. Bonham, E. Miñones-Moyano, A. J. Moreno, D. Wang, K. Chang, G. Williams, B. I. Garay, I. Lobach, N. Devidze, D. Kim, C. Anderson-Bergman, G.-Q. Yu, C. C. White, J. A. Harris, B. L. Miller, D. A. Bennett, A. P. Arnold, P. L. D. Jager, J. J. Palop, B. Panning, J. S. Yokoyama, L. Mucke, D. B. Dubal, A second X chromosome contributes to resilience in a mouse model of Alzheimer's disease, *Sci. Transl. Med.* **12** (2020), doi:10.1126/scitranslmed.aaz5677.

51. A. Agostini, D. Yuchun, B. Li, D. A. Kendall, M.-C. Pardon, Sex-specific hippocampal metabolic signatures at the onset of systemic inflammation with lipopolysaccharide in the APPswe/PS1dE9 mouse model of Alzheimer's disease, *Brain. Behav. Immun.* **83**, 87–111 (2020).

52. N. J. Izzo, C. Yuede, K. LaBarbera, C. Limegrover, C. Rehak, R. Yurko, L. Waybright, G. Look, G. Rishton, H. Safferstein, M. Hamby, C. Williams, K. Sadlek, H. Edwards, C. Davis, M. Grundman, L. Schneider, S. T. DeKosky, D. Chelsky, I. Pike, C. M. Henstridge, K. Blennow, H. Zetterberg, LeVine III, Harry, T. L. Spires-Jones, J. Cirrito, S. M. Catalano, Preclinical and Clinical Biomarker Studies of CT1812: A Novel Approach to Alzheimer's Disease, *Alzheimers Dement. N. Y. N* **In press** (2021).

53. F. Bartz, L. Kern, D. Erz, M. Zhu, D. Gilbert, T. Meinhof, U. Wirkner, H. Erfle, M. Muckenthaler, R. Pepperkok, H. Runz, Identification of Cholesterol-Regulating Genes by Targeted RNAi Screening, *Cell Metab.* **10**, 63–75 (2009).

54. T. J. Montine, C. H. Phelps, T. G. Beach, E. H. Bigio, N. J. Cairns, D. W. Dickson, C. Duyckaerts, M. P. Frosch, E. Masliah, S. S. Mirra, P. T. Nelson, J. A. Schneider, D. R. Thal, J. Q. Trojanowski, H. V. Vinters, B. T. Hyman, National Institute on Aging, Alzheimer's Association, National Institute on Aging-Alzheimer's Association guidelines for the neuropathologic assessment of Alzheimer's disease: a practical approach, *Acta Neuropathol. (Berl.)* **123**, 1–11 (2012).

55. H. Braak, I. Alafuzoff, T. Arzberger, H. Kretzschmar, K. Del Tredici, Staging of Alzheimer disease-associated neurofibrillary pathology using paraffin sections and immunocytochemistry, *Acta Neuropathol. (Berl.)* **112**, 389–404 (2006).

56. D. R. Thal, U. Rüb, M. Orantes, H. Braak, Phases of A beta-deposition in the human brain and its relevance for the development of AD, *Neurology* **58**, 1791–1800 (2002).

57. J. Schindelin, I. Arganda-Carreras, E. Frise, V. Kaynig, M. Longair, T. Pietzsch, S. Preibisch, C. Rueden, S. Saalfeld, B. Schmid, J.-Y. Tinevez, D. J. White, V. Hartenstein, K. Eliceiri, P. Tomancak, A. Cardona, Fiji: an open-source platform for biological-image analysis, *Nat. Methods* **9**, 676–682 (2012).

58. C. A. Schneider, W. S. Rasband, K. W. Eliceiri, NIH Image to ImageJ: 25 years of image analysis, *Nat. Methods* **9**, 671–675 (2012).

59. M. Colom-Cadena, J. Pegueroles, A. G. Herrmann, C. M. Henstridge, L. Muñoz, M. Querol-Vilaseca, C. S. Martín-Paniello, J. Luque-Cabecerans, J. Clarimon, O. Belbin, R. Núñez-Llaves, R. Blesa, C. Smith, C.-A. McKenzie, M. P. Frosch, A. Roe, J. Fortea, J. Andilla, P. Loza-Alvarez, E. Gelpi, B. T. Hyman, T. L. Spires-Jones, A. Lleó, Synaptic phosphorylated α-synuclein in dementia with Lewy bodies, *Brain* **140**, 3204–3214 (2017).

60. F. S. Wouters, P. J. Verveer, P. I. Bastiaens, Imaging biochemistry inside cells, *Trends Cell Biol.* **11**, 203–211 (2001).

61. R Core Team, R: a language and environment for statistical computing (2017) (available at https://www.R-project.org/).

Acknowledgments

The authors thank our brain tissue donors and their families for their generous donations. Authors gratefully acknowledge membership of Edinburgh Neuroscience. Some of the control participants in the human study were from the Lothian Birth Cohort 1936, thus we wish to thank the cohort and research team supported by Age UK (Disconnected Mind project) in The University of Edinburgh Centre for Cognitive Ageing and Cognitive Epidemiology, funded by the Biotechnology and Biological Sciences Research Council (BBSRC) and Medical Research Council (MRC) ((MR/K026992/1).

Author contributions

T.S.J, J.T., S.C., N.I., M.C.C., conceived, designed, and/or planned the experiments; M.C.C., performed human cases experiments; J.T., R.J.J., M.H. C.D, M.T., handled and dosed mice; J.H.C. S.D., R.T. A.A.F., stained and analysed mice data; T.S.J., M.C.C, prepared the manuscript; J.T.,

R.J.J., J.H.C, J.R., C.D., M.H., A.A.F., S.D., R.T., M.T., N.I., S.C., C.S., C.S., contributed and critically reviewed the manuscript.

Funding

This work was supported by Alzheimer's Society (project grant AS-PG-15b-023), Alzheimer's Research UK, the European Research Council (ERC) under the European Union's Horizon 2020 research and innovation programme (Grant agreement No. 681181), the University of Edinburgh (Chancellor's Fellow start-up funding), Wellcome Trust Institutional Strategic Support Fund, the UK Dementia Research Institute which receives its funding from DRI Ltd., funded by the UK Medical Research Council, Alzheimer's Society, and Alzheimer's Research UK, and BBSRC Institute Strategic Programme funding.

Competing interests

TSJ is a member of the scientific Advisory Board of Cognition Therapeutics. NI and SC are employees of Cognition Therapeutics.

Data and materials availability

All data associated with this study are available in the main text or the supplementary materials.